(12)

AD

TECHNICAL REPORT ARLCB-TR-83043

FRACTURE BEHAVIOR OF A URANIUM AND A TUNGSTEN ALLOY IN A NOTCHED COMPONENT WITH INERTIA LOADING

J. H. UNDERWOOD

M. A. SCAVULLO

DECEMBER 1983

US ARMY ARMAMENT RESEARCH AND DEVELOPMENT CENTER
LARGE CALIBER WEAPON SYSTEMS LABORATORY
BENÉT WEAPONS LABORATORY
WATERVLIET N.Y. 12189

DISCLAIMER

The findings in this report are not to be construed as an official Department of the Army position unless so designated by other authorized documents.

The use of trade name(s) and/or manufacture(s) does not constitute an official indorsement or approval.

DISPOSITION

Destroy this report when it is no longer needed. Do not return it to the originator.

SECURITY CLASSIFICATION OF THIS PAGE (When Data Entered)

REPORT DOCUMENTATION PAGE

READ INSTRUCTIONS BEFORE COMPLETING FORM

1. REPORT NUMBER: ARLCB-TR-83043	2. GOVT ACCESSION NO.: AD-A139649
3. RECIPIENT'S CATALOG NUMBER	
4. TITLE (and Subtitle): FRACTURE BEHAVIOR OF A URANIUM AND A TUNGSTEN ALLOY IN A NOTCHED COMPONENT WITH INERTIA LOADING	5. TYPE OF REPORT & PERIOD COVERED: Final
	6. PERFORMING ORG. REPORT NUMBER
7. AUTHOR(s): J. H. Underwood and M. A. Scavullo	8. CONTRACT OR GRANT NUMBER(s)
9. PERFORMING ORGANIZATION NAME AND ADDRESS: US Army Armament Research & Development Center, Benet Weapons Laboratory, DRSMC-LCB-TL, Watervliet, NY 12189	10. PROGRAM ELEMENT, PROJECT, TASK AREA & WORK UNIT NUMBERS: AMCMS No. 6126.03.H180.0, PRON No. 1A325B461A1A
11. CONTROLLING OFFICE NAME AND ADDRESS: US Army Armament Research & Development Center, Large Caliber Weapon Systems Laboratory, Dover, NJ 07801	12. REPORT DATE: December 1983
	13. NUMBER OF PAGES: 29
14. MONITORING AGENCY NAME & ADDRESS(if different from Controlling Office)	15. SECURITY CLASS. (of this report): UNCLASSIFIED
	15a. DECLASSIFICATION/DOWNGRADING SCHEDULE

16. DISTRIBUTION STATEMENT (of this Report)

Approved for public release; distribution unlimited.

17. DISTRIBUTION STATEMENT (of the abstract entered in Block 20, if different from Report)

18. SUPPLEMENTARY NOTES

Presented at Sixteenth National Symposium on Fracture Mechanics, ASTM, Columbus, Ohio, 15-18 August 1983.
Published in proceedings of the symposium.

19. KEY WORDS (Continue on reverse side if necessary and identify by block number)

Uranium Alloy
Tungsten Alloy
Brittle Fracture
Nondestructive Inspection
Stress Analysis

20. ABSTRACT (Continue on reverse side if necessary and identify by block number)

A failure of a prototype long rod penetrator is described, including the stress and fracture analyses performed, the materials and service simulation testing performed, and the fracture toughness and nondestructive inspection requirements which were implemented.

Results of a subsequent study are described, which involve the producibility of the long rod penetrator, particularly in relation to the complex fracture toughness testing methods which are required for use with this component.

DD FORM 1 JAN 73 1473 EDITION OF 1 NOV 65 IS OBSOLETE

UNCLASSIFIED

SECURITY CLASSIFICATION OF THIS PAGE (When Data Entered)

TABLE OF CONTENTS

TABLES

Page

LIST OF ILLUSTRATIONS

INTRODUCTION, PROBLEM, OBJECTIVES

Described here is an elastic stress-controlled fracture of a specialized, cannon-launched projectile, a so-called kinetic energy projectile. The general outline of such a projectile is shown in Figure 1, as a finite element mesh. It consists of two components, a solid cylinder long rod penetrator and a sabot which attaches to the penetrator and propels it out of the cannon. The penetrator is made from high density, high strength material, typically a tungsten or uranium alloy, so that it can effectively penetrate armor by means of its own kinetic energy. The sabot is made from a low density material, an aluminum alloy, so that it consumes as little kinetic energy as possible. The interconnection between penetrator and sabot is a series of lugs which are the same in cross-section as buttress threads, but have no helical advance.

The fracture problem is that, on occasion, the tail of a prototype penetrator has fallen off during launch of the projectile. Both the tungsten and the uranium alloys used for penetrators are relatively brittle materials, and certain locations of the penetrator are subjected to high tensile stress during launch. Failures have occurred with one early prototype uranium penetrator and with two prototype tungsten penetrators. All failures have occurred at the same location, the root of the rearmost lug, as shown in Figure 1. As was shown by subsequent stress analysis, this is the location of the highest axial tensile stress in the penetrator during launch.

The objectives of this report are twofold. We describe the failure analysis and related implementations, which have apparently prevented any further brittle failures in this type of component. We also describe a subsequent producibility analysis which indicates that some simplification of

the rigorous fracture mechanics tests can be made with no significant loss of reliability, but with an improvement in producibility of the component.

STRESS ANALYSIS

The stress analysis, a requisite for failure analysis, was based on two separate finite element models. Details of the models are given in prior work (ref 1). An overview is given here. Figure 1 shows the model of the projectile, both penetrator and sabot. The elastic and yield properties of the two penetrator materials and the sabot material vary considerably (see Table I) and have considerable effects on the model results. The uranium alloy is solution-treated and aged; the tungsten alloy is a liquid-phase sintered product. The elastic stresses due to launch loading were obtained for all areas of penetrator and sabot, with special interest and a higher element density near the location of the prototype failures. The stresses at this location were primarily the result of the projectile acceleration which acted on the mass of the tail portion of the penetrator behind this location. An additional loading condition was a limit on the force transfer between sabot and penetrator. This simulated the limitation of the shear stress in the sabot lugs to the shear yield stress of the aluminum alloy used for the sabot.

---

[1]G. A. Pflegl, J. H. Underwood, and G. P. O'Hara, "Structural Analysis of a Kinetic Energy Projectile During Launch," US ARRADCOM Report No. ARLCB-TR-81028, Benet Weapons Laboratory, Watervliet, NY, July 1981.

In order to analyze the failure at the root of the lug, a second finite element model was constructed of an individual lug (refs 1,2). The stresses from the first whole-projectile model were used as input to the second lug model. For the uranium alloy, both elastic and elastic-plastic analyses were performed using the lug model.

Figure 2 and Table II summarize key results from the two models. The plot in Figure 2 is the distribution of axial direction elastic stresses from elements nearest the outer diameter of the whole-projectile model. The launch pressure and related acceleration are those associated with the uranium prototype failure. Note that the model predicts an increasing axial stress which peaks over 400 MPa tension near the rearmost lug. A similar increasing stress distribution can be predicted from the following simple analysis of the overhanging tail section of the penetrator:

$$\sigma_z = p + \frac{wG}{A} \qquad (1)$$

in which σ_z is the average axial stress at a given location in the tail section; p is the launch pressure, 225 MPa; $w = \ell A\mu$ is the weight of the portion of tail section of length ℓ and area A; μ is the weight density of the uranium alloy, 0.187 MN/m^3; G is the relative acceleration, 34,400, unitless, relative to gravitational acceleration. The plot of Eq. (1) gives a first order approximation for the combined effects of pressure and acceleration on

---

[1]G. A. Pflegl, J. H. Underwood, and G. P. O'Hara, "Structural Analysis of a Kinetic Energy Projectile During Launch," US ARRADCOM Report No. ARLCB-TR-81028, Benet Weapons Laboratory, Watervliet, NY, July 1981.

[2]G. P. O'Hara, "Elastic-Plastic Analysis of Screw Threads," US ARRADCOM Report ARLCB-TR-80043, Benet Weapons Laboratory, Watervliet, NY, November 1980.

the tail section of the penetrator.

Results of the stress analysis are listed in Table II for both the lug root radius of the current design, ρ = 0.3 mm, and a much larger radius, ρ = 1.1 mm, which would be possible with a significant redesign of the lug. The nominal axial stress, σ_z, at the location of the rearmost lug was obtained from plots such as Figure 2. Elastic stress concentration factors, K_t, for the lug roots were obtained from the single-lug model (refs 1,2). The total elastic stress at the lug root is the sum of the concentrated axial stress $\sigma_z \cdot K_t$, and the additional lug root stress due to the cantilever-bending-type loading of the lug. Comparing results of Tables I and II, it can be seen that the total elastic lug root stress is above the yield strength for the larger ρ and above the ultimate strength for the smaller ρ. Elastic-plastic analysis with the single-lug model resulted in lug root stresses between the yield and ultimate strengths. These values of lug root stress, σ_R, were used in the fracture analysis.

FRACTURE ANALYSIS

The basic equation used to calculate critical defect sizes at the lug root is:

$$K_I = f\ \sigma\ (\pi a)^{1/2} \qquad (2)$$

in which K_I is the opening mode stress intensity factor; σ is the local

---

[1] G. A. Pflegl, J. H. Underwood, and G. P. O'Hara, "Structural Analysis of a Kinetic Energy Projectile During Launch," US ARRADCOM Report No. ARLCB-TR-81028, Benet Weapons Laboratory, Watervliet, NY, July 1981.

[2] G. P. O'Hara, "Elastic-Plastic Analysis of Screw Threads," US ARRADCOM Report ARLCB-TR-80043, Benet Weapons Laboratory, Watervliet, NY, November 1980.

stress, in this case at the notch root; a is the crack depth; and f is the dimensionless factor which accounts for the relative crack depth, in relation to the rod radius, r, and the surface crack length, 2c, in this case. Referring to K solutions from compendia, it can be shown that f is primarily dependent on crack shape, a/2c in the case of the relatively brittle materials and associated shallow cracks to be dealt with here. The limiting value of f for shallow cracks with a/2c → 0 is quite generally a constant 1.12, whereas for shallow surface cracks with a nonzero a/2c, f varies considerably with a/2c and a/2c is the controlling parameter for shallow surface cracks. A crack shape of a/2c = 0.3 is typical for material cracks and is the worst that could be expected for the case here. A lower value of a/2c might be expected if the metal forming processes for the rod caused elongation of the circumferential direction, the direction of the 2c surface length for the defect orientation of concern. However, it is the axial direction of the rod which is elongated in metal forming. Therefore, assuming a worst case semi-elliptical defect at the lug root with a/2c = 0.3, a in the radial direction, 2c in the circumferential direction, gives an f value of 0.83 (ref 3). Using this value and rewriting Eq. (2) gives an expression for critical defect size, a_c:

$$a_c = 0.462\ (K_{Ic}/\sigma_R)^2 \qquad (3)$$

in which K_{Ic} is the plane-strain fracture toughness of the material and σ_R is lug root stress from Table II. Measurements of K_{Ic} were taken from the early

---

[3]D. P. Rooke and D. J. Cartwright, Compendium of Stress Intensity Factors, Her Majesty's Stationery Office, London, 1976, p. 298.

prototype material and the recent process material, both at -46°C, as shown in Table III. Using values of toughness at two standard deviations below mean, alarmingly small critical defect sizes were predicted; see again Table II.

IMPLEMENTATIONS

Fracture Toughness and Nondestructive Inspection

An important implementation of the results of the stress and fracture analyses was the setting of requirements for fracture toughness and defect size for uranium penetrators. The key results are listed in Table IV. One penetrator blank in a heat treat lot is used for K_{Ic} measurement, and the finish-machined penetrators are inspected for defects using an eddy current method. Following the setting of these requirements, no brittle failure of a uranium penetrator has occurred during launch loading.

Launch Simulation Testing

It was decided early in this investigation to develop a means to simulate the launch stresses on finish-machined penetrators. The main reason for such launch simulation was the relatively low fracture toughness of the penetrator materials and the associated small defect size. A service simulation test which could be performed on the critical component in its final condition would provide a complement to the toughness and nondestructive inspection requirements. Such a service simulation test is shown in Figure 3. The test applies load to the penetrator in the same general way as that of launch, that is, by way of fixtures which interconnect with the lugs in the same way as the sabot. The connecting fixtures, called sabot sections, are made of high strength steel. One section loads the lug faces which are 7° from the normal

to the penetrator axis. These are the same faces loaded in launch. The other sabot section loads 45° lug faces and takes advantage of the significant compressive stress component of such loading. This has prevented failure of the penetrator during simulation tests at the location of the 45° face sabot section, except for one unexplained instance. In all other tests the failure occurred at the root of the rearmost lug loaded on the 7° face, as shown in Figure 3. The deflection of the specimen and fixture assembly is measured as shown. Load versus deflection plots of the worst and the best tungsten and uranium penetrators which have been loaded to failure are seen in Figure 4. Note that although the fracture load of the best tungsten penetrator slightly exceeds that of the worst uranium test, the failure energy, defined as area under the curve, separates the two materials. The failure energy of even the worst uranium test is significantly above that of the best tungsten test.

The launch simulation test was used to evaluate a group of suspect penetrators, the K_{Ic} of which often fell below the required 33 $MPa \cdot m^{1/2}$ minimum. Two penetrators from each of five heat treat lots were tested in launch simulation. Two to four K_{Ic} tests from each of the five heat treat lots were performed. The plot of failure energy from the launch simulation test versus K_{Ic} is shown in Figure 5. Note that K_{Ic} values above 37 $MPa \cdot m^{1/2}$ are invalid because of insufficient crack length; see ASTM Method E399-83, Plane-Strain Fracture Toughness of Metallic Materials. The resulting linear correlation coefficient, 0.93, indicates that low fracture toughness and low launch simulation failure energy are clearly related to one another.

Design Modifications to Reduce Stress

For future designs of penetrators, modifications from the current geometry should be implemented where possible in order to reduce lug root stress. Some guidance for the more significant design modifications can be obtained from the work here. In order to quantify the effects of the modifications, three proposed modifications were identified, and it was assumed that a factor of two change from the baseline geometry was possible for each modification. Then the results described here were used to calculate the decrease in lug root stress relative to that of the baseline geometry. See Table V.

The first modification listed, to increase the lug root radius, is an obvious approach, and its effect can be quantified using the following expression:

$$\frac{K_{t1}}{K_{t2}} = \left(\frac{\rho_2}{\rho_1}\right)^n \tag{4}$$

in which n is a constant exponent and K_t and ρ are as described in Table II. Equation (4) states that the variation of K_t with ρ is an inverse exponential relation. Using the values of K_t and ρ in Table II, n = 0.26. Using this value of n, it can be easily shown that a factor two increase in ρ, from 0.3 to 0.6 mm, results in a reduction in root stress by a ratio of 0.84.

A second and also obvious modification in design in order to reduce penetrator stress is a decrease in the penetrator overhang, that is, the length of penetrator rearward of the sabot. Equation (1) can be used in slightly different form to quantify the effect of this modification:

$$\sigma_z = p + \ell\mu G \tag{5}$$

This expression, with all parameters as in Eq. (1), gives the average axial direction normal stress at the rear of the sabot with a length ℓ of penetrator overhanging rearward. Using ℓ = 0.088, the nominal overhang of the penetrator in the baseline design, and half that value, gives a significant reduction in stress, a ratio of 0.17, as a result of a factor of two decrease in overhang.

A third modification in order to reduce penetrator stress is a decrease in the stiffness of the sabot. Specifically, if the section thickness were reduced at the tapered rear projection of the sabot (see Figure 1), then the loading which is transferred through the sabot and penetrator lugs to the penetrator lug root would be reduced. The approximate effect on lug root stress of such a reduction in sabot stiffness can be calculated as:

$$\text{stress reduction ratio} = \frac{\sigma_z \cdot K_t + 0.5\ \sigma_{\text{lug load}}}{\sigma_{\text{total}}} \qquad (6)$$

Using values of 1150, 680, and 1830 MPa from Table II for $\sigma_z \cdot K_t$, $\sigma_{\text{lug load}}$, and σ_{total}, respectively, the reduction in stress is a ratio of 0.81. This reduction corresponds to the removal of one-half of the loading on the penetrator lug due to a decrease in sabot stiffness.

It is clear that the effects of the above three modifications are correct only for the particular idealized situations which were described. However, the analyses do provide clear guidance for implementing future design changes in order to prevent fracture of penetrators.

PRODUCIBILITY

The producibility of a component such as the penetrator considered here is primarily dependent on its configuration and the manufacturing processes

involved. However, the fracture toughness requirements can affect the overall producibility of the component, particularly for materials as brittle as the uranium and tungsten alloys considered here. Simpler fracture tests increase producibility. Fracture testing and analysis were performed for the two materials with the objective of replacing the relatively complex K_{Ic} test with a simpler test which still gives an adequate measure of toughness under the conditions of the service loading.

Uranium

The results given here in Table II and Figure 5 show that: (a) the uranium penetrator has such low toughness and small critical defect size that K_{Ic} has significant control over its structural integrity; (b) the failure energy of a uranium penetrator under simulated service loading is directly related to K_{Ic}. These results indicate that direct measurement of K_{Ic} is justified for the uranium penetrator. A simpler fracture test procedure which could be considered is a demonstration that a notched-energy-to-failure test correlates closely with K_{Ic}. Then the simpler, non-precracked test can be used as an indirect measure of K_{Ic}, in the same general way that the Charpy impact test is used with some steels.

Tungsten

The testing and analyses of tungsten penetrators centered on fourteen penetrators which were loaded to failure in the launch simulation test, as shown in Figure 3. The failure energies measured from the tests were clearly divided into two groups, a group of five with mean failure energy of 381 Nm, and a group of nine with a mean of 1126 Nm. These fourteen penetrators, with a large range of failure energy which clearly separated good from bad, were

used to test the ability of tensile and fracture tests to separate good from bad.

Tensile elongation is sometimes used to specify tungsten alloys. Tensile specimens of two sizes were made from the remains of the failure energy tests. Figures 6 and 7 show how tensile elongation and reduction-in-area related to failure energy for the smaller of the tensile specimens. All tensile test results are summarized in Table VI. Note the considerable variation in tensile elongation measurements from the smaller specimens, as indicated by the low correlation coefficient in Figure 6 and by the standard deviation which is larger than the mean value in Table VI. The results in general show that reduction-in-area is better than tensile elongation for correlation with failure energy, and the larger tensile specimens give the lesser variation.

A slow notched bend energy test was also performed from specimens made from remains of the failure energy tests. A sketch of the test specimen and arrangement is shown in Figure 8. The total strain energy input to the specimen until failure was measured by calculating the area under the load versus mid-point deflection curve. Two notch depths were used. The specimen with the shallower notch, 2 mm, was the same as the v-notch Charpy impact specimen of ASTM Method E23-82, Notched Bar Impact Testing of Metallic Materials. The only significant difference in the test performed here is that the time to peak load was about ten seconds rather than a fraction of a millisecond as in impact testing. Figure 9 shows the results of tests with the 2 mm deep notch. All the slow notched bend energy results are summarized in Table VI. The correlation of slow notched bend energy with failure energy is slightly better for the deeper notch, whereas the variation of slow notched

bend energy is slightly worse for the deeper notch, based on the high energy group data.

The fracture toughness results showed the least variation of all tests performed and correlated better with failure energy than any other set of results. It should be noted that one of three critical validity requirements for K_{Ic} tests was not met for three of the six tests performed; see ASTM Method E399-83. With the Charpy size specimens used, the maximum-to-offset load ratio requirement, less than 1.1, was met, as was the test specimen thickness requirement. The specimen crack length requirement was not satisfied for critical K values above 49 $MPa \cdot m^{1/2}$, which included the three results from the high energy group.

SUMMARY

The failure of both uranium and tungsten penetrators due to actual or simulated inertia-loading of cannon launch is significantly controlled by plane-strain fracture toughness. However, since the critical defect size in both materials is so small and difficult to characterize, the total energy to failure of the actual component provides a better measure of structural integrity than traditional fracture mechanics.

Plane-strain fracture toughness is the preferred material specification test, because it correlates better with failure energy and has less variability than any of the tensile and fracture tests investigated. However, as is often the case, the complexity of K_{Ic} testing is a disadvantage for a high-production component. A simpler slow notched bend energy test gives a reliable prediction of failure energy and the associated structural integrity

in service for tungsten penetrators. Initial results indicate that the slow notched bend energy test would give at least an adequate prediction of failure energy for uranium penetrators.

REFERENCES

1. G. A. Pflegl, J. H. Underwood, and G. P. O'Hara, "Structural Analysis of a Kinetic Energy Projectile During Launch," US ARRADCOM Report No. ARLCB-TR-81028, Benet Weapons Laboratory, Watervliet, NY, July 1981.
2. G. P. O'Hara, "Elastic-Plastic Analysis of Screw Threads," US ARRADCOM Report No. ARLCB-TR-80043, Benet Weapons Laboratory, Watervliet, NY, November 1980.
3. D. P. Rooke and D. J. Cartwright, Compendium of Stress Intensity Factors, Her Majesty's Stationery Office, London, 1976, p. 298.

TABLE I. MATERIALS AND ROOM TEMPERATURE PROPERTIES

	Yield Strength MPa	Tensile Strength MPa	Elastic Modulus MPa	Fracture Toughness $MPa \cdot m^{1/2}$
Uranium, 0.75 Titanium	830	1450	170,000	55
Tungsten, 7.0 Nickel, 3.0 Iron	1100	1150	310,000	69
Aluminum; 7075-T6	620	670	70,000	20

TABLE II. STRESS AND FRACTURE ANALYSIS OF URANIUM PENETRATOR

	Notch Root Radius, ρ = 0.3 mm	Notch Root Radius, ρ = 1.1 mm
Nominal axial stress, σ_z; at -46°C	410 MPa	410 MPa
Elastic stress concentration factor, K_t	2.8	2.0
Notch root stress; elastic		
$\sigma_z \cdot K_t$	1150 MPa	820 MPa
Lug loading	680 MPa	410 MPa
Total	1830 MPa	1230 MPa
Notch root stress; elastic-plastic		
Total; σ_R	1280 MPa	1100 MPa
Critical defect size, a_c; at -46°C		
for K_{Ic} = 17.5 $MPa \cdot m^{1/2}$	0.09 mm	0.12 mm
for K_{Ic} = 34.4 $MPa \cdot m^{1/2}$	0.33 mm	0.45 mm

TABLE III. FRACTURE TOUGHNESS MEASUREMENTS OF URANIUM AT -46°C

Material	Number of Tests	Mean K_{Ic}, $MPa \cdot m^{1/2}$	Standard Deviation, S $MPa \cdot m^{1/2}$	$K_{Ic}-2S$ $MPa \cdot m^{1/2}$
Prototype	9	23.9	3.2	17.5
Recent	9	38.2	1.9	34.4

TABLE IV. FRACTURE TOUGHNESS AND NONDESTRUCTIVE INSPECTION REQUIREMENTS FOR URANIUM PENETRATOR

Fracture Toughness, Minimum Required at -46°C	NDI Requirements at Lug Root		
	location	depth	surface length
33 $MPa \cdot m^{1/2}$	Rearmost 5 lugs	0.25 mm	1.5 mm

TABLE V. SUMMARY OF PROCEDURES TO REDUCE LUG ROOT STRESS

Procedure	Factor	Effect; Ratio of Reduced to Original Stress
Increase root radius	x 2	0.84 (Eq. 4)
Decrease penetrator overhang	x 2	0.17 (Eq. 5)
Decrease sabot stiffness	x 2	0.81 (Eq. 6)

TABLE VI. TENSILE AND FRACTURE TEST RESULTS FOR TUNGSTEN AT ROOM TEMPERATURE

Test	Mean and Standard Deviation		Number of Tests	Correlation With Failure Energy
	Low Energy Group	High Energy Group		
Failure Energy	381 Nm; 103 Nm	1126 Nm; 101 Nm	14	-
Tensile Elongation				
3.2 mm diameter	3.8%; 4.6%	8.6%; 2.4%	12	+0.68
4.1 mm diameter	2.6%; 0.7%	14.4%; 3.1%	10	+0.88
Reduction in Area				
3.2 mm diameter	3.7%; 2.3%	16.4%; 6.1%	12	+0.77
4.1 mm diameter	4.2%; 0.2%	21.3%; 5.5%	10	+0.82
Slow Notched Bend Energy				
2 mm notch	0.86 Nm; 0.38 Nm	2.26 Nm; 0 38 Nm	11	+0.91
3 mm notch	0.41 Nm; 0.11 Nm	1.18 Nm; 0.47 Nm	10	+0.94
Fracture Toughness	41 MPa$\cdot$m$^{1/2}$; 4 MPa$\cdot$m$^{1/2}$	69 MPa$\cdot$m$^{1/2}$; 3 MPa$\cdot$m$^{1/2}$	6	+0.98

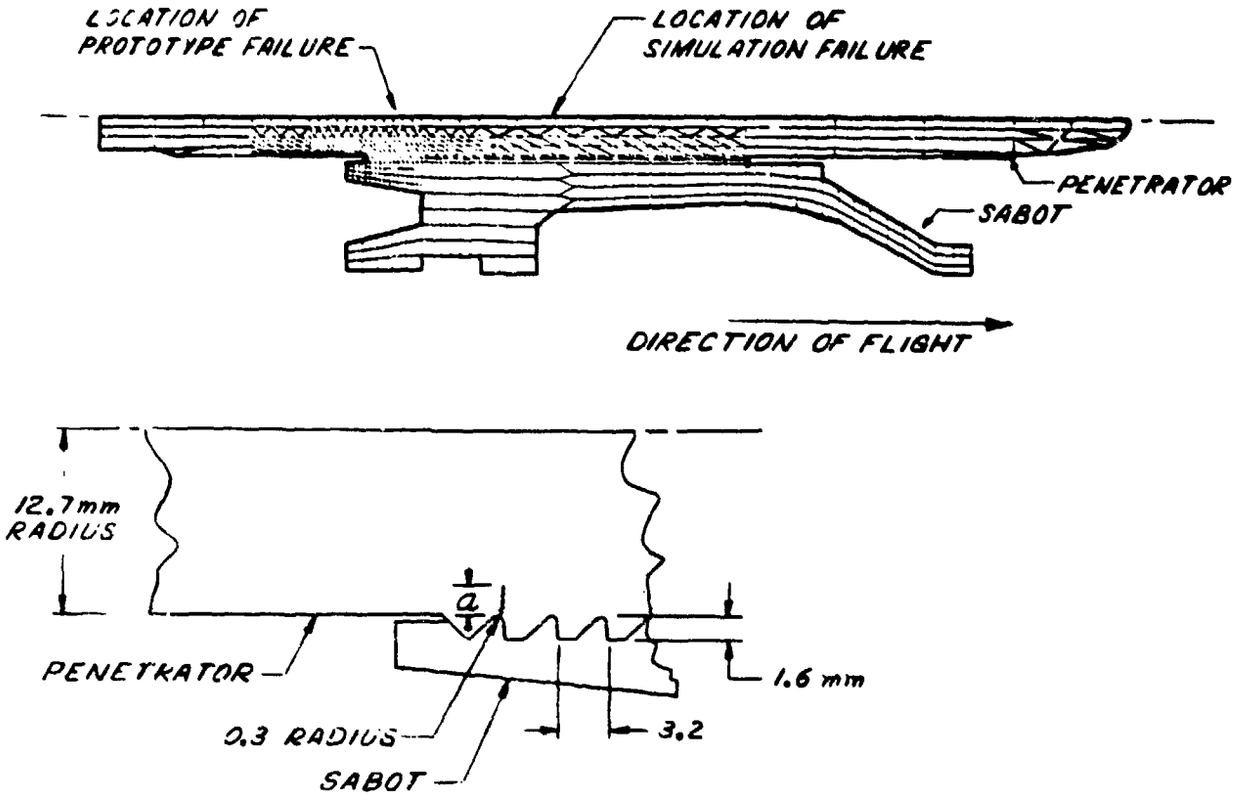

Figure 1. Finite Element Model of Long Rod Kinetic Energy Penetrator and Sabot; Sketch of Prototype Failure Location.

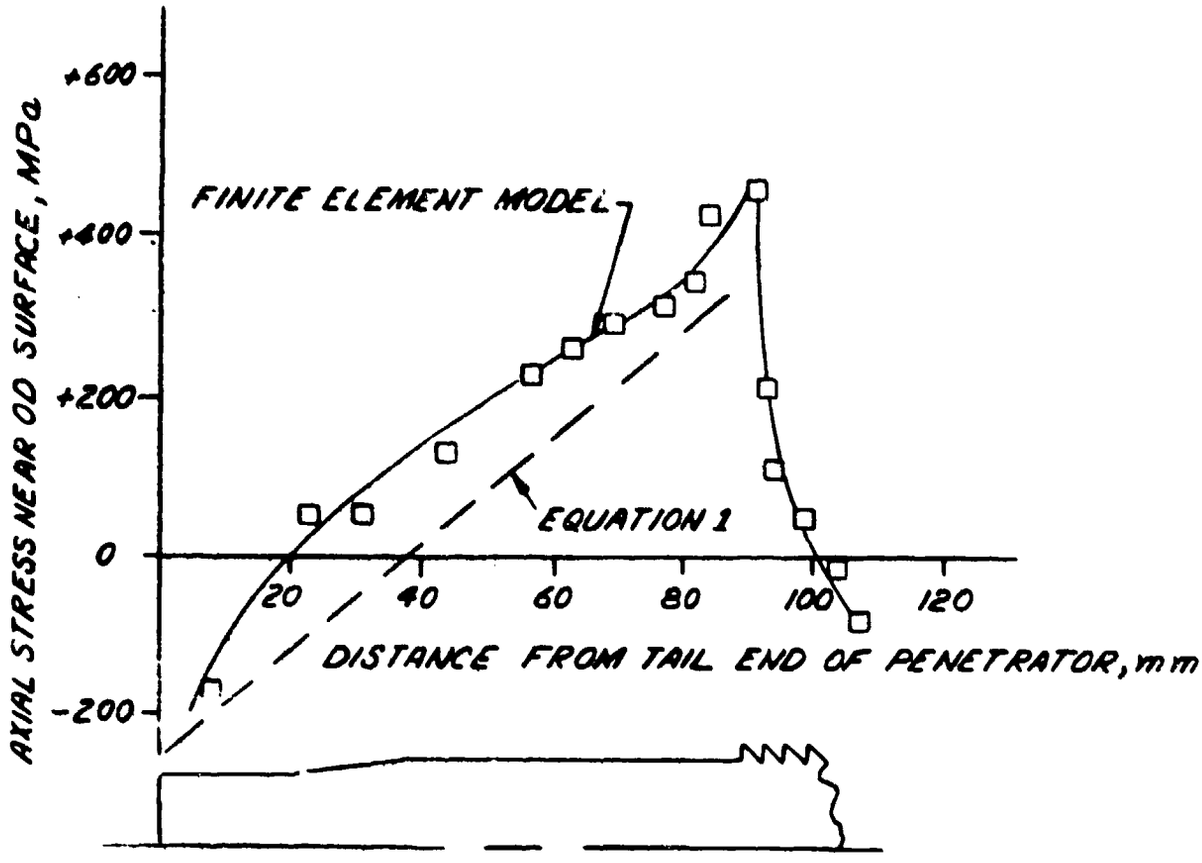

Figure 2. Axial Stress Distribution Near OD of Tail End of Uranium Penetrator for 225 MPa Pressure Applied.

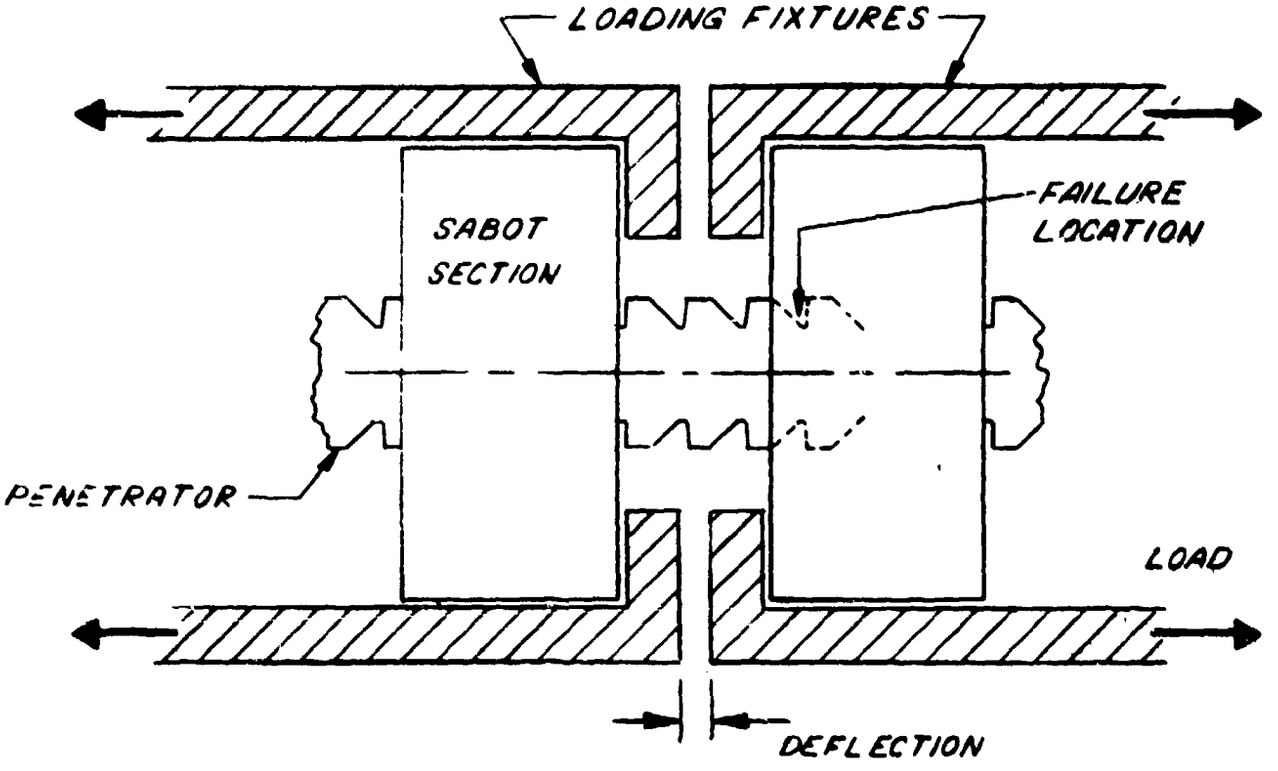

Figure 3. Sketch of Launch Loading Simulation Test.

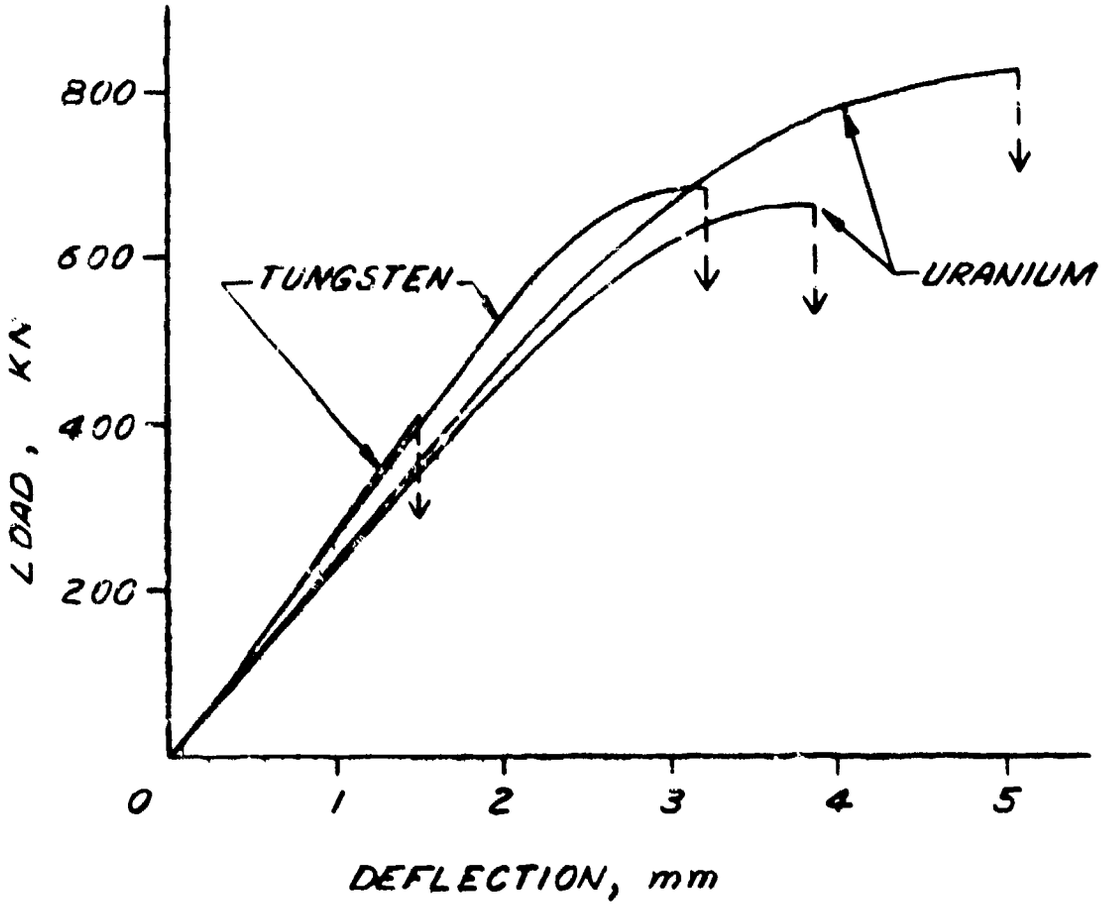

Figure 4. Launch Loading Simulation Tests of Tungsten and Uranium Penetrators; Highest and Lowest Energy to Failure Tests.

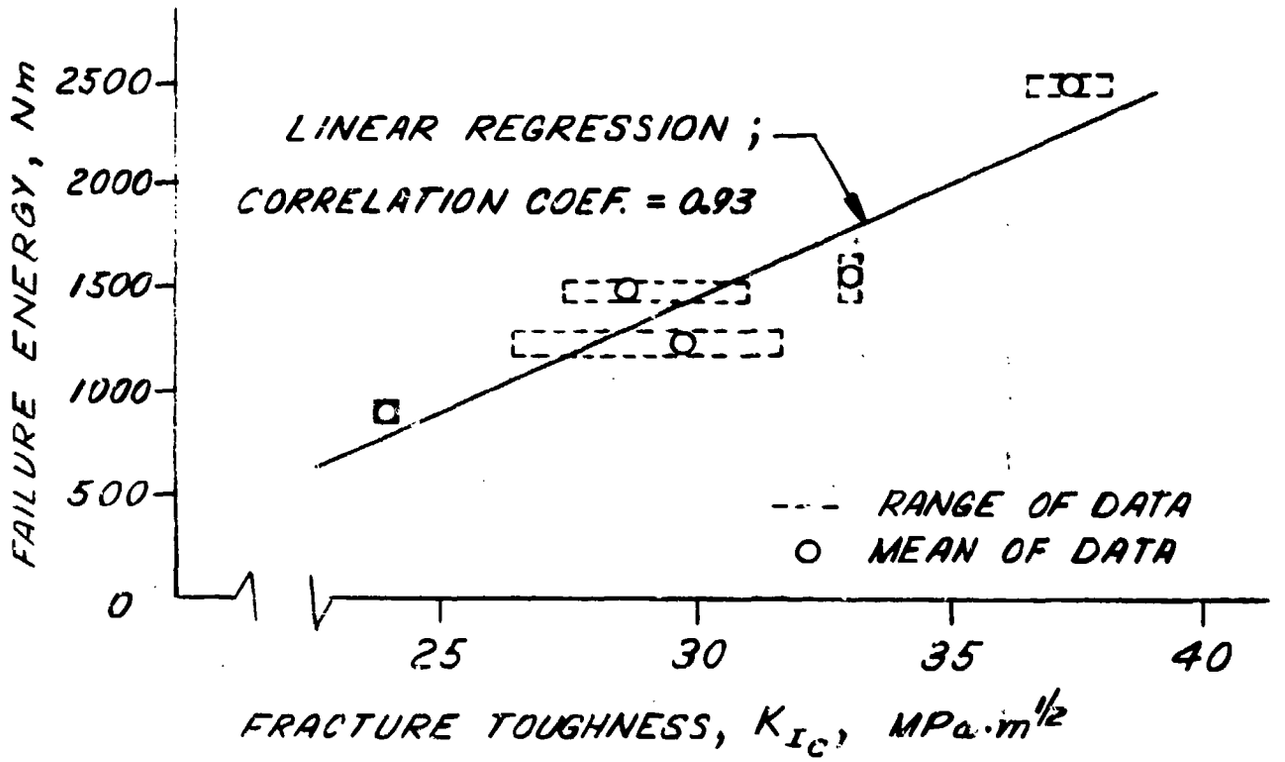

Figure 5. Relation Between Room Temperature Failure Energy and -46°C Fracture Toughness for Uranium.

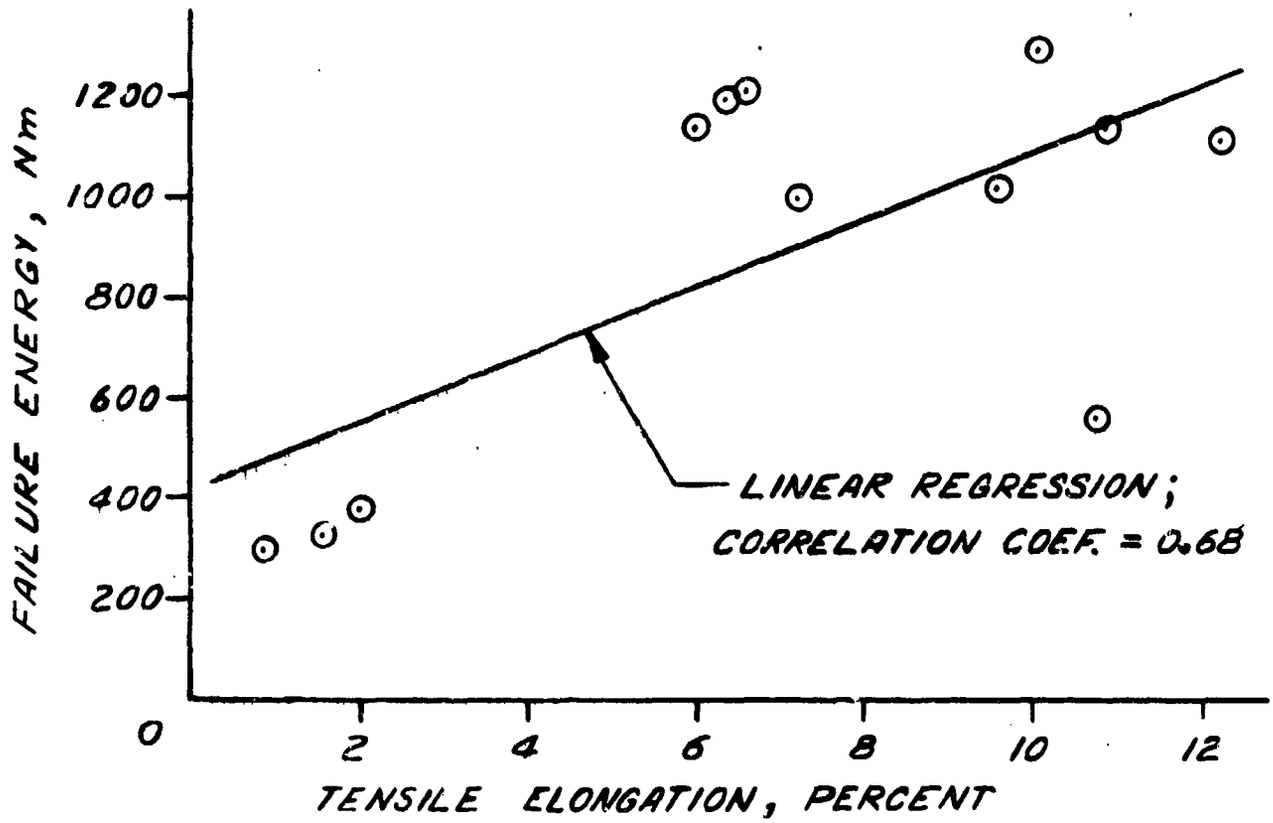

Figure 6. Relation Between Failure Energy and Tensile Elongation Using 3.2 mm Diameter Tensile Specimen; for Tungsten at Room Temperature.

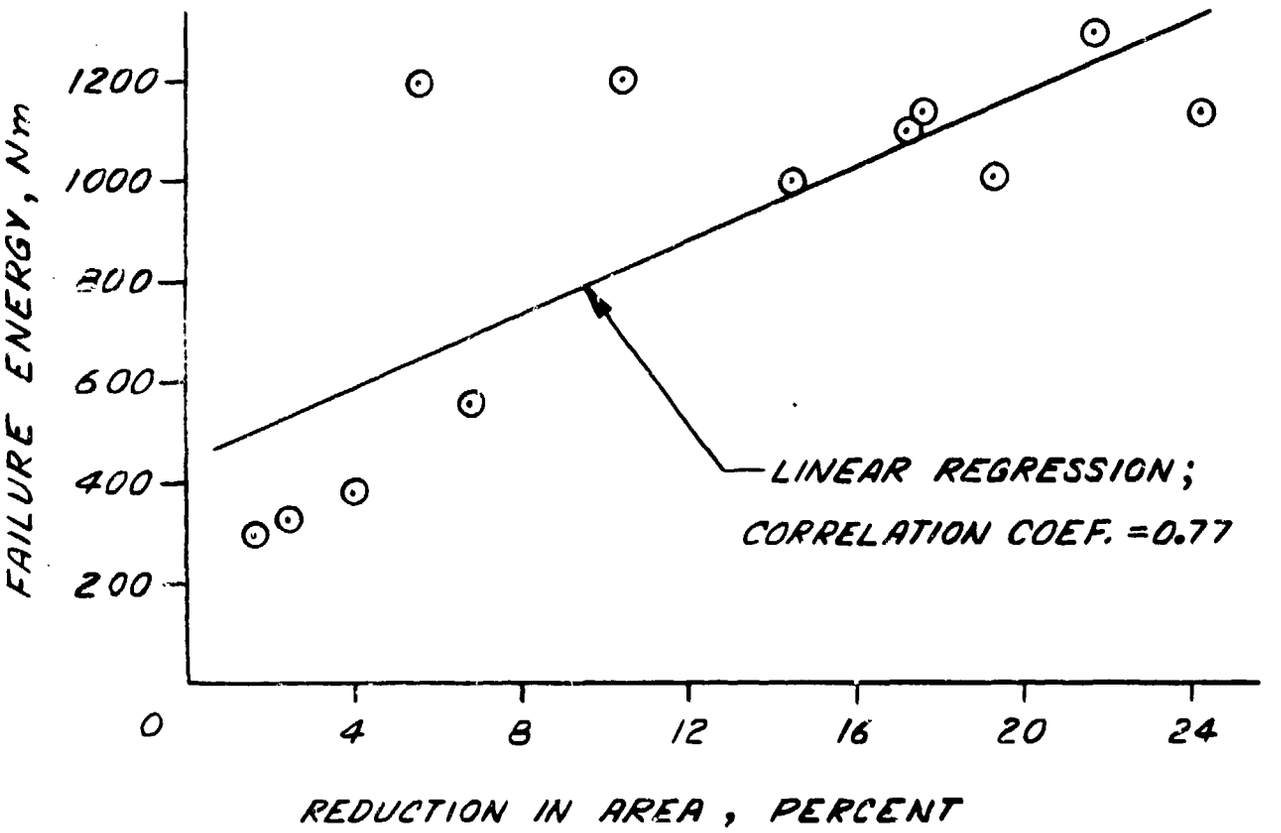

Figure 7. Relation Between Failure Energy and Reduction-in-Area Using 3.2 mm Diameter Tensile Specimen; for Tungsten at Room Temperature.

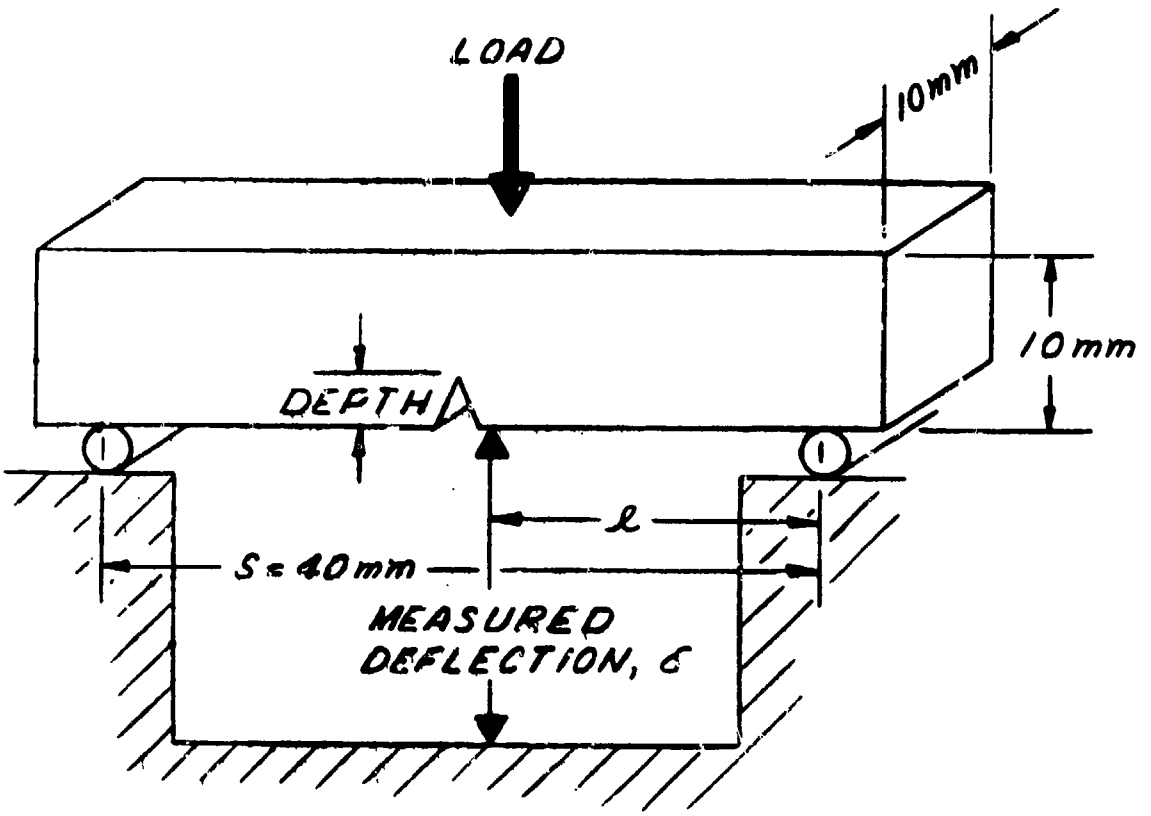

Figure 8. Sketch of Slow Notched Bend Energy Test.

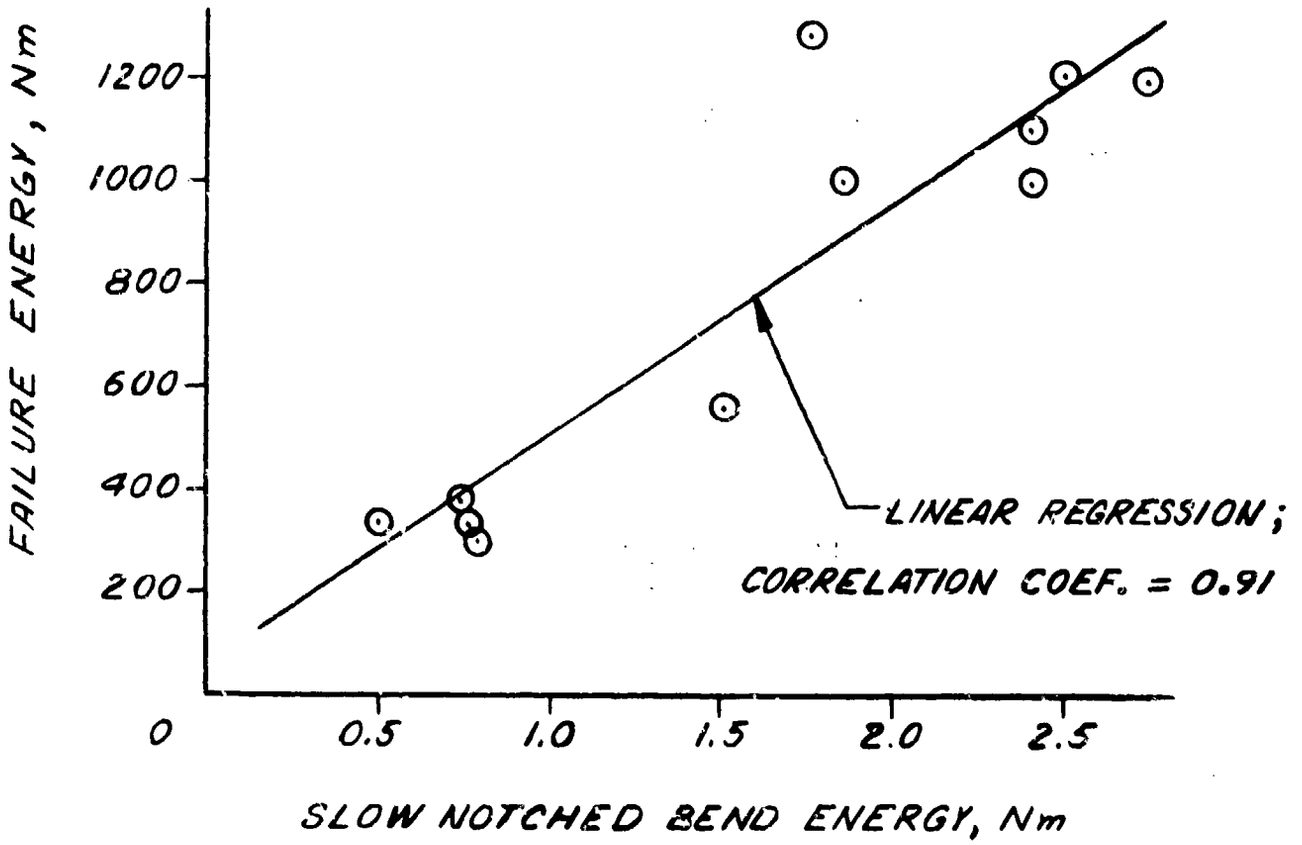

Figure 9. Relation Between Failure Energy and Slow Notched Bend Energy Using 2 mm Deep Notch; for Tungsten at Room Temperature.

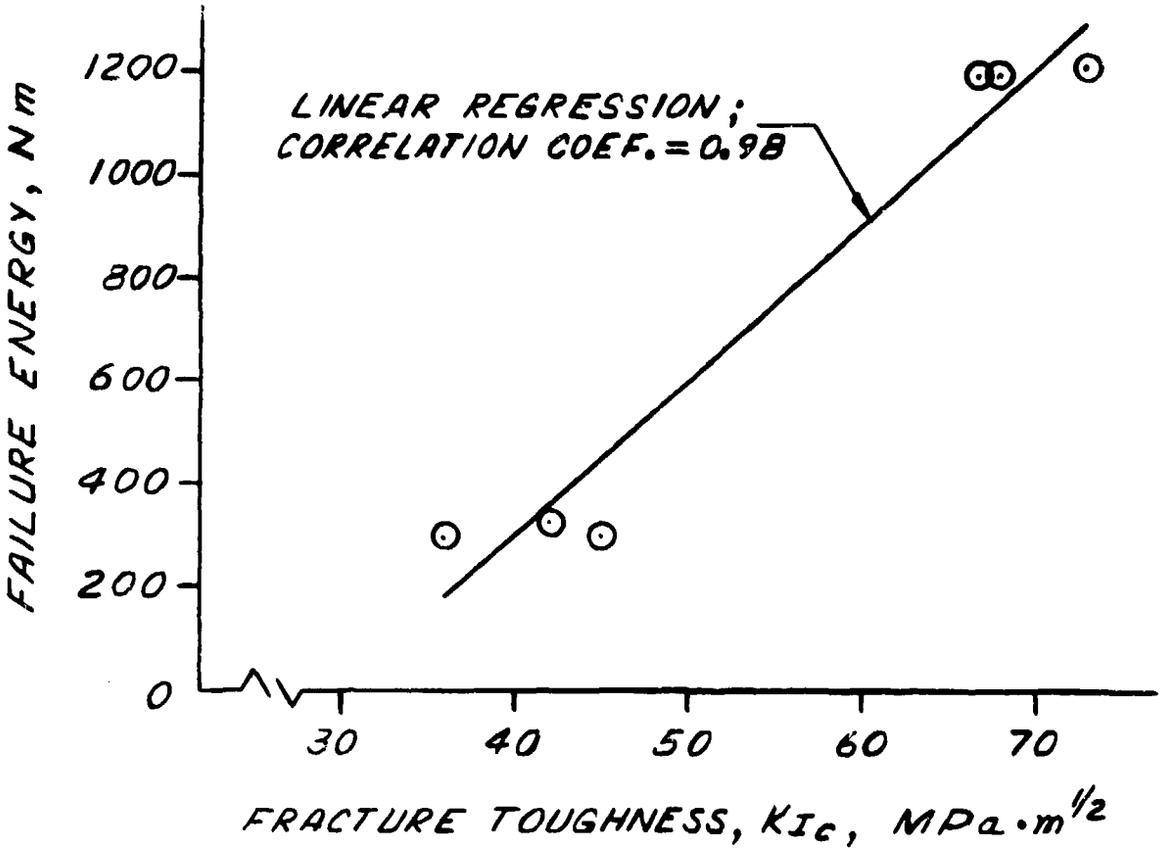

Figure 10. Relation Between Failure Energy and Fracture Toughness; for Tungsten at Room Temperature.

TECHNICAL REPORT INTERNAL DISTRIBUTION LIST

	NO. OF COPIES
CHIEF, DEVELOPMENT ENGINEERING BRANCH	
ATTN: DRSMC-LCB-D	1
-DP	1
-DR	1
-DS (SYSTEMS)	1
-DS (ICAS GROUP)	1
-DC	1
CHIEF, ENGINEERING SUPPORT BRANCH	
ATTN: DRSMC-LCB-S	1
-SE	1
CHIEF, RESEARCH BRANCH	
ATTN: DRSMC-LCB-R	2
-R (ELLEN FOGARTY)	1
-RA	1
-RM	1
-RP	1
-RT	1
TECHNICAL LIBRARY ATTN: DRSMC-LCB-TL	5
TECHNICAL PUBLICATIONS & EDITING UNIT ATTN: DRSMC-LCB-TL	2
DIRECTOR, OPERATIONS DIRECTORATE	1
DIRECTOR, PROCUREMENT DIRECTORATE	1
DIRECTOR, PRODUCT ASSURANCE DIRECTORATE	1

NOTE: PLEASE NOTIFY DIRECTOR, BENET WEAPONS LABORATORY, ATTN: DRSMC-LCB-TL, OF ANY ADDRESS CHANGES.

TECHNICAL REPORT EXTERNAL DISTRIBUTION LIST

	NO. OF COPIES
ASST SEC OF THE ARMY RESEARCH & DEVELOPMENT ATTN: DEP FOR SCI & TECH THE PENTAGON WASHINGTON, D.C. 20315	1
COMMANDER DEFENSE TECHNICAL INFO CENTER ATTN: DTIC-DDA CAMERON STATION ALEXANDRIA, VA 22314	12
COMMANDER US ARMY MAT DEV & READ COMD ATTN: DRCDE-SG 5001 EISENHOWER AVE ALEXANDRIA, VA 22333	1
COMMANDER ARMAMENT RES & DEV CTR US ARMY AMCCOM	
ATTN: DRSMC-LC(D)	1
DRSMC-LCE(D)	1
DRSMC-LCM(D) (BLDG 321)	1
DRSMC-LCS(D)	1
DRSMC-LCU(D)	1
DRSMC-LCW(D)	1
DRSMC-SCM-O (PLASTICS TECH EVAL CTR, BLDG. 351N)	1
DRSMC-TSS(D) (STINFO)	2
DOVER, NJ 07801	
DIRECTOR BALLISTICS RESEARCH LABORATORY ARMAMENT RESEARCH & DEV CTR US ARMY AMCCOM ATTN: DRSMC-TSB-S (STINFO) ABERDEEN PROVING GROUND, MD 21005	1
MATERIEL SYSTEMS ANALYSIS ACTV ATTN: DRSXY-MP ABERDEEN PROVING GROUND, MD 21005	1
COMMANDER US ARMY AMCCOM ATTN: DRSMC-LEP-L(R) ROCK ISLAND, IL 61299	1
COMMANDER ROCK ISLAND ARSENAL ATTN: SMCRI-ENM (MAT SCI DIV) ROCK ISLAND, IL 61299	1
DIRECTOR US ARMY INDUSTRIAL BASE ENG ACTV ATTN: DRXIB-M ROCK ISLAND, IL 61299	1
COMMANDER US ARMY TANK-AUTMV R&D COMD ATTN: TECH LIB - DRSTA-TSL WARREN, MI 48090	1
COMMANDER US ARMY TANK-AUTMV COMD ATTN: DRSTA-RC WARREN, MI 48090	1
COMMANDER US MILITARY ACADEMY ATTN: CHMN, MECH ENGR DEPT WEST POINT, NY 10996	1
US ARMY MISSILE COMD REDSTONE SCIENTIFIC INFO CTR ATTN: DOCUMENTS SECT, BLDG. 4484 REDSTONE ARSENAL, AL 35898	2
COMMANDER US ARMY FGN SCIENCE & TECH CTR ATTN: DRXST-SD 220 7TH STREET, N.E. CHARLOTTESVILLE, VA 22901	1

NOTE: PLEASE NOTIFY COMMANDER, ARMAMENT RESEARCH AND DEVELOPMENT CENTER, US ARMY AMCCOM, ATTN: BENET WEAPONS LABORATORY, DRSMC-LCB-TL, WATERVLIET, NY 12189, OF ANY ADDRESS CHANGES.

TECHNICAL REPORT EXTERNAL DISTRIBUTION LIST (CONT'D)

	NO. OF COPIES
COMMANDER US ARMY MATERIALS & MECHANICS RESEARCH CENTER ATTN: TECH LIB - DRXMR-PL WATERTOWN, MA 01272	2
COMMANDER US ARMY RESEARCH OFFICE ATTN: CHIEF, IPO P.O. BOX 12211 RESEARCH TRIANGLE PARK, NC 27709	1
COMMANDER US ARMY HARRY DIAMOND LAB ATTN: TECH LIB 2800 POWDER MILL ROAD ADELPHIA, MD 20783	1
COMMANDER NAVAL SURFACE WEAPONS CTR ATTN: TECHNICAL LIBRARY CODE X212 DAHLGREN, VA 22448	1

	NO. OF COPIES
DIRECTOR US NAVAL RESEARCH LAB ATTN: DIR, MECH DIV CODE 26-27, (DOC LIB) WASHINGTON, D.C. 20375	1 1
COMMANDER AIR FORCE ARMAMENT LABORATORY ATTN: AFATL/DLJ AFATL/DLJG EGLIN AFB, FL 32542	1 1
METALS & CERAMICS INFO CTR BATTELLE COLUMBUS LAB 505 KING AVENUE COLUMBUS, OH 43201	1

NOTE: PLEASE NOTIFY COMMANDER, ARMAMENT RESEARCH AND DEVELOPMENT CENTER, US ARMY AMCCOM, ATTN: BENET WEAPONS LABORATORY, DRSMC-LCB-TL, WATERVLIET, NY 12189, OF ANY ADDRESS CHANGES.

READER EVALUATION

Please take a few minutes to complete the questionnaire below and return to us at the following address: Commander, Armament Research and Development Center, U.S. Army AMCCOM, ATTN: Technical Publications, DRSMC-LCB-TL, Watervliet, NY 12189.

1. Benet Weapons Lab. Report Number _____

2. Please evaluate this publication (check off one or more as applicable).

	Yes	No
Information Relevant	____	____
Information Technically Satisfactory	____	____
Format Easy to Use	____	____
Overall, Useful to My Work	____	____

Other Comments _____

_____

_____

3. Has the report helped you in your own areas of interest? (i.e. preventing duplication of effort in the same or related fields, savings of time, or money). _____

_____

_____

4. How is the report being used? (Source of ideas for new or improved designs. Latest information on current state of the art, etc.). _____

_____

_____

5. How do you think this type of report could be changed or revised to improve readability, usability? _____

_____

_____

6. Would you like to communicate directly with the author of the report regarding subject matter or topics not covered in the report? If so please fill in the following information.

Name: _____

Telephone Number: _____

Organization Address: _____

_____